Stress-Induced $\gamma \rightarrow \alpha'$ Martensitic Transformation in Two Carbon Stainless Steels. Application to Trip Steels

FRANCOIS ABRASSART

The influence of the temperature θ_a of a prestraining of austenite above M_d on the subsequent stress-induced $\gamma \rightarrow \alpha'$ transformation in the (M_s, M_d) range is examined in two carbon stainless steels. It is shown that the yield stress, which is controlled by the transformation, increases with θ_a at given testing temperature and amount of prestraining. This behavior is related to the influence of θ_a on the nature and arrangement of the defects present in austenite after the prestraining: planar defects (*i.e.*, stacking faults, twins, ϵ platelets) predominate if θ_a is close to M_d whereas undissociated dislocation cells are only to be observed if θ_a if higher. This is consistent with the strong increase of the intrinsic stacking fault energy of the austenite, as inferred from measurements using the node method on a hot stage microscope. In addition, the ability of plane defects to propagate under stress is shown to be lower after a prestraining at higher θ_a, which is attributed to a segregation of impurity atoms on dislocations. It is concluded that the nucleation stress of the $\gamma \rightarrow \alpha'$ transformation is the stress necessary to allow planar defects to propagate in the prestrained austenite.

SINCE its discovery by Scheil,[1] the phenomenon of stress-induced martensitic transformation above M_s has led to a great number of investigations on various types of steels.

If the temperature is low enough, the transformation, which is a deformation mode, can even "control" the yield stress of the steel: the transformation starts exactly at the beginning of the plastic deformation and the yield stress is notably lower than when transformation does not occur; the result is an abnormal positive yield stress-temperature sensitivity.

In their attempts to develop a new class of strong and ductile steels, (TRIP steels), Zackay *et al.*[2,7] were confronted with this problem: in spite of a plastic prestraining of austenite at a temperature θ_a higher than M_d, the low temperature yield stress stays rather low in the case of a too high instability of austenite towards transformation.

Moreover, the strong influence of the nature and arrangement of defects in austenite upon the nucleation processes of the spontaneous and stress-induced transformations is well known.

In the case of stainless steels, the spontaneously quench-induced martensite volume fraction after a prestraining at temperature θ_a is higher if the intrinsic stacking fault energy (SFE) of austenite at θ_a is lower.[8]

More precisely, stainless steels have made it possible to observe a peculiar type of association between defects in austenite and both spontaneous and stress-induced α' martensites. In these alloys, the SFE of austenite is rather low so that mechanical twinning[9-12] and $\gamma \rightarrow \epsilon$ martensitic transformation[5,9-18] are modes of plastic deformation. The latter transformation may also be spontaneous.[9,13,16,19-23,25] Although it has been suggested that the $\gamma \rightarrow \epsilon$ transformation is a mode of accommodation of internal stresses generated by the $\gamma \rightarrow \alpha'$ transformation,[20,21,23] it seems more realistic to consider ϵ, in a number of steels, as being an intermediate product of $\gamma \rightarrow \alpha'$, as may be inferred from the geometry of the ϵ-α' association, especially when α' is present at the intersection of two ϵ platelets.[9-13,18,19,24]

The role of intermediary played by ϵ is generally thought to arise from the fact that a lattice structure very close to martensite can be produced by a $a/6$ $\langle 112 \rangle_\gamma$ shear every two $(111)_\gamma$ planes: this shear is precisely that which leads to the formation of ϵ martensite. A second homogeneous shear of ϵ would then produce the bcc structure.[9,13,24,26,27] Unfortunately, this theory neglects the dislocation mechanisms responsible for the second shear; besides, it might imply that α' martensite would preferentially nucleate on preexisting ϵ platelets (this will be referred to in the following as "static nucleation").

On the contrary, Lecroisey[11,12] has proposed a mechanism explaining the creation and propagation of transformation dislocations $a/18 \langle 112 \rangle_\gamma$ when two plane defects produced during plastic deformation (twins, ϵ platelets, stacking faults) come to an intersection. According to him, the very high local stresses necessary to allow the propagation of these dislocations can exist at the instant of intersection only: thus the nucleation process would be dynamic; this dynamic nature had already been suggested by other authors.[6,13] However, the processes involved still remain unclear.

In spite of the great amount of work dealing with the defect-transformation interaction, the peculiar influence of a prestraining of austenite above M_d on the subsequent stress-induced $\gamma \rightarrow \alpha'$ transformation in the (M_s, M_d) range is still unknown. In particular, we believe that the yield stress in this temperature range will depend, if "controlled" by the transformation, on the θ_a temperature of this prestraining, since θ_a itself conditions the nature and arrangement of defects introduced in austenite. We will verify this fact in two car-

FRANÇOIS ABRASSART is Research Engineer, IRSID, Saint-Germain-en-Laye, France. This work is part of a thesis prepared at the Centre des Matériaux de l'Ecole des Mines, Corbeil, France, and submitted at the University of Nancy, June 1972.

Manuscript submitted December 18, 1972.

bon stainless steels, one synthetic, the other commercial.

From a practical point of view, these steels, which are similar to TRIP steels, will permit us to determine the θ_a temperature which results in the highest yield stresses between M_s and M_d.

From a more fundamental point of view, the relationships between stress, defects and $\gamma \rightarrow \alpha'$ transformation will be considered and the nature of the nucleation process, either static or dynamic, will be discussed. For this purpose, we have successively studied:

1) The intrinsic stacking fault energy of the austenite as a function of temperature.

2) The modes of plastic deformation in the austenite above M_d.

3) The influence of the prestraining temperature θ_a of austenite on the volume fraction of spontaneous $\gamma \rightarrow \alpha'$ transformation below M_s.

4) The influence of θ_a on the yield stress between M_s and M_d and on the stress-induced $\gamma \rightarrow \alpha'$ transformation.

EXPERIMENTAL PROCEDURE

1. Materials

The compositions of the steels are given in Table I.

Steel 1 was specially designed for the purpose of this study. Ingots of approximately 2 kg were prepared by induction melting in an argon atmosphere from metals of electrolytic purity. After about 50 pct reduction by hot rolling, the ingots were homogenized 72 h at 1150°C in an argon atmosphere. Then they were rolled into plates of about 7 mm thick. Round tensile specimens were cut from these plates. After machining, the specimens were given an austenitizing treatment of 30 min at 1090°C in evacuated Vycor capsules, producing a grain size of about 100 μm and complete dissolution of carbides.

Steel 2 is a commercial steel, delivered in the as-quenched condition as bars of 12 mm diam. Specimens were only given an austenitizing treatment of 30 min at 1050°C in an argon atmosphere, producing a grain size of about 30 μm.

2. Transformation Temperatures

Three methods were used to determine the M_s $\gamma \rightarrow \alpha'$ temperature: differential dilatometry, magnetic measurements and optical microscopy. The accuracy of M_s is estimated to be ±5°C. The M_d $\gamma \rightarrow \alpha'$ temperature was determined by the continuous measurement of the intensity of magnetization during tensile tests (see below).

The ϵ phase has proved to be difficult to detect because the volume fraction transformed is very low; since martensite is paramagnetic,[9] magnetic measurements are impossible. We then used an X-ray diffractometer with a hot stage. $A_F^{\gamma \rightarrow \epsilon}$, the temperature of the end of the $\epsilon \rightarrow \gamma$ transformation on heating, could only be measured by this method.

Table I. Composition of the Alloys, Wt Pct

	C	Cr	Ni	Mo	Mn	Si	Al	Nb
Steel 1	0.18	18	7					
Steel 2	0.13	15.5	4.2	2.7	1.2	0.16	0.17	0.10

3. Metallography

The structures were observed by optical and electron microscopy (Philips EM 300) on flat specimens (1 mm by 5 mm by 50 mm).

4. Intrinsic Stacking Fault Energy of Austenite

The intrinsic stacking fault energy was measured from the observation of triple nodes. The measurements were only possible on Steel 1, Steel 2 being too unstable towards $\gamma \rightarrow \alpha'$ transformation in thin foil. The sheets were lightly deformed in tension (2 pct) to produce fresh dislocations. The influence of temperature above RT on the node sizes was studied by means of the Philips hot stage microscope. No observations were possible above 350°C because of oxidation of the specimens. We applied the result of Brown's calculations with $\nu = 0.3$; $b_s = 1.46$Å; $\mu = 7.4 \times 10^{11}$ d per sq cm; $1/\mu \times d\mu/d\theta = -7 \times 10^{-4}$ per deg C.[11,12]

5. Mechanical Properties

Cylindrical tensile specimens of 3 mm diam and 32 mm gage length were tested with an Instron TTDM machine. The deformation rate was set at 10^{-3} s^{-1}. A coil furnace was used for specimens deformed at temperature above 250°C. Below this temperature, the specimens were tested in liquid baths allowing a homogeneous temperature controlled to ±2°C in the range (−196°C, +250°C).

6. Magnetic Measurements

We designed a double coil device, described elsewhere,[34] allowing a continuous measurement of the intensity of magnetization J of the specimens, assumed proportional to the volume fraction M of α' martensite formed during plastic deformation. This device can also be used for static measurements (extraction method).

EXPERIMENTAL RESULTS

1. Steel 1

1.1 ALLOY STRUCTURE IN THE QUENCHED CONDITION AND TRANSFORMATION TEMPERATURES

Two distinct transformations, $\gamma \rightarrow \epsilon$ and $\gamma \rightarrow \alpha'$, were observed in this alloy.

1) $\gamma \rightarrow \epsilon$ Transformation. The structure of the steel quenched to RT and observed through optical microscopy is characterized by the presence in some grains of parallel-sided platelets similar to the ϵ platelets observed by many authors in stainless steels (Fig. 1(a)). Electron microscopy confirms this interpretation (Fig. 1(b-c)). $A_F^{\gamma \rightarrow \epsilon}$ seems to be located at about 250°C, as may be inferred from the disappearance of the $(10.1)_\epsilon$ line (RX measurements, Fig. 2). However, as will be seen, specimens deformed 20 pct at various θ_a temperatures do not contain any ϵ martensite (and/or twins) at RT when $\theta_a \geq 200$°C. Then $A_F^{\gamma \rightarrow \epsilon} \leq 200$°C.

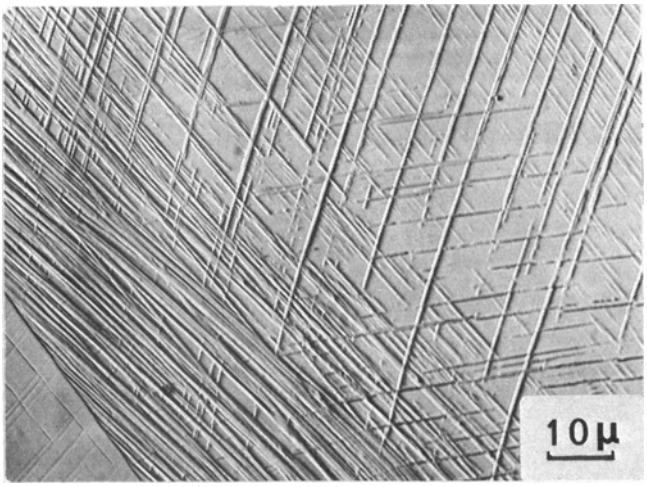

(a)

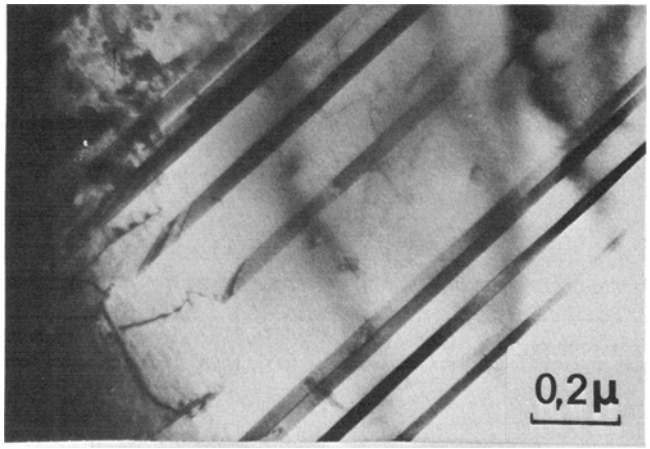

(b)

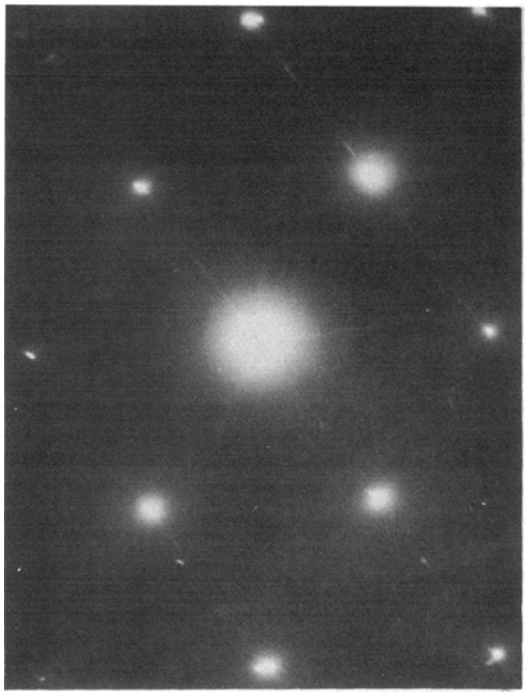

(c)

Fig. 1—Steel 1 in quenched condition, (*a*) ϵ martensite; (*b*, *c*) ϵ martensite and corresponding (110) diffraction pattern.

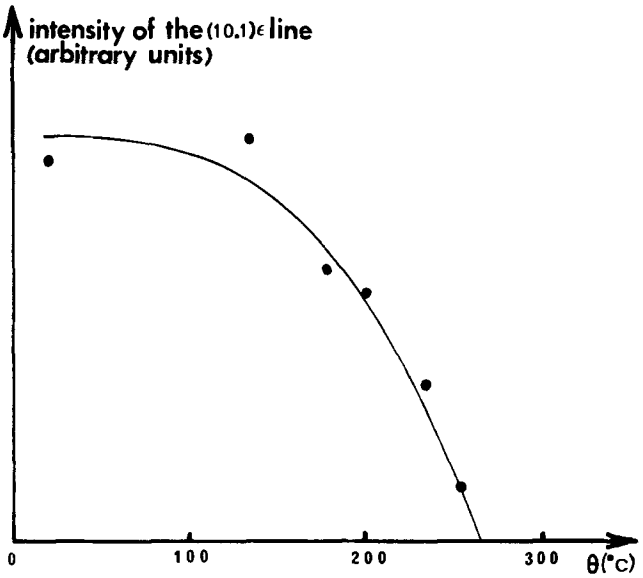

Fig. 2—Steel 1: Reversion of ϵ martensite on heating, X-ray measurements.

The difference might be explained by the presence, in the first case, of an ϵ martensite which, being related to superficial α' martensite, is expected to be more stable.

ii) $\gamma \rightarrow \alpha'$ Transformation. Optical microscopy allows to observe α' martensite after a quench to −70°C. This martensite is closely associated to ϵ martensite (Fig. 3(*a*)). This type of morphology is widely documented.[11,13,19-21,26,27,35]

Such α' martensite is often located at the intersection of two ϵ platelets (Fig. 3(*b*)). Differential dilatometry shows and qualitative magnetic tests (with a strong hand magnet) confirm that M_s is situated at about −80°C.

Thus, $\gamma \rightarrow \epsilon$ and $\gamma \rightarrow \alpha'$ martensitic transformations occur in two partially distinct temperature ranges in this steel. M_d temperature is situated between 80 and 90°C.

1.2 INTRINSIC STACKING FAULT ENERGY MEASUREMENTS

i) SFE Measurements at RT. These measurements were performed on 42 nodes observed in 11 different thin foils. One of these nodes is shown in Fig. 4. The results are presented in Fig. 5(*a*) where each square stands for one measurement. The maximum of the diagram is located between 18 and 19 ergs per sq cm, which is a rather low SFE and is close to the values measured on Fe-18 Cr-8 Ni steels, say 15 to 20 ergs per sq cm.[36,37]

ii) Influence of Temperature above RT. The following method was used. Each convenient triple node was observed at increasing temperatures (20, 120, 200, 330°C). The temperature was allowed to stabilize (between 15 and 30 min) before nodes were photographed. Then the thin foil was cooled down by switching off the hot stage heating current and a micrograph of the nodes was taken again at RT. 18 nodes belonging to 7 different thin foils were observed. An example of the variation in node size over a thermal cycle is shown in Fig. 4 and Fig. 5(*b*) represents the variations of measured ("apparent") SFE.

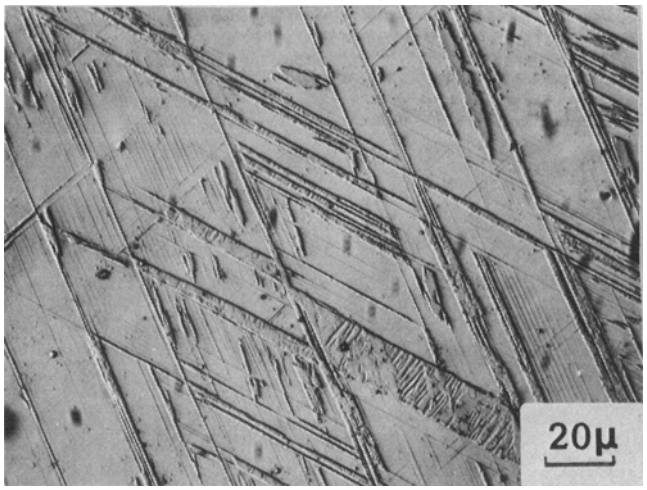

(a)

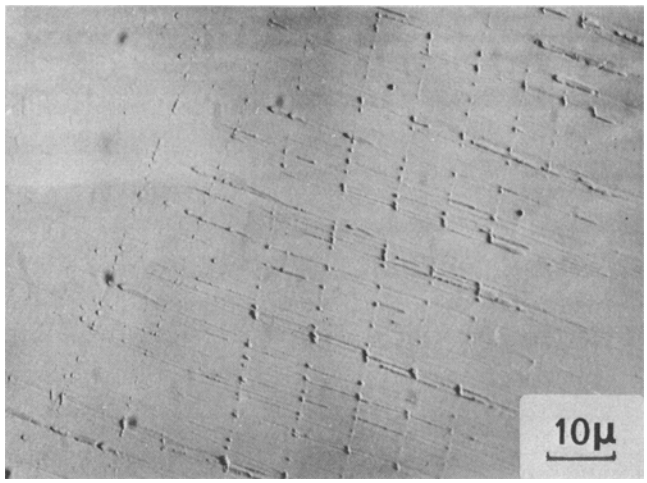

(b)

Fig. 3—Steel 1: Spontaneous $\gamma \rightarrow \alpha'$ transformation after a quench to −196°C (*a*) general morphology; (*b*) $\gamma \rightarrow \alpha'$ transformation at intersections of ϵ platelets.

The SFE (f) increases rapidly with temperature: $df/d\theta \simeq 0.1$ erg per sq cm per deg C, which is in agreement with recent results obtained on stainless steels.[11,12,40,41] The scatter of the results also increases with increasing temperature. This can be explained, at least partially, by an increasing uncertainty with decreasing node size. The dimensions of the nodes decrease with a remarkable continuity during this heating.

After cooling down to RT, the apparent SFE is much higher than at the beginning of the cycle and the scatter is very large. As we will see later, the observed irreversibility is thought to be due to a segregation phenomenon on dislocations. Since this segregation is dependent on the cycling conditions which are difficult to control (aging time $\theta(t)$ and heating rate $d\theta/dt$), the observed scatter is not surprising. The evolution of node sizes is not so regular on cooling as on heating: rapid extensions can be seen to take place, especially below 100°C. Finally, the lower stability of austenite towards transformation in thin foils, as compared with stability in bulk specimens, did not allow accurate SFE measurements below RT to be made. However, it was possible to detect a rapid increase of node sizes during further cooling.

1.3 MODES OF PLASTIC DEFORMATION IN AUSTENITE ABOVE M_d. INFLUENCE OF TEMPERATURE

Those modes of deformation are strongly dependent upon the temperature θ_a of deformation. Specimens of Steel 1 were strained (ϵ_a = 20 pct) at θ_a = 110, 150, 200, 350, and 500°C. These temperatures being higher than M_d, the steel stays fully austenitic. The structures of these various conditions are shown in the micrographs of Figs. 6 and 7 such as they are observed at RT.

When $\theta_a \geq$ 200°C, no twins, ϵ platelets or stacking faults are detected by optical or electron microscopy (Fig. 6(*a-b*)). Slip lines and equiaxed dislocation cells typical of a high SFE are only to be seen. Moreover, this structure proves to be very stable when the temperature is lowered on the cooling stage of the electron microscope: stacking faults propagate rarely above −100°C and their extension is very limited; many regions remain unaltered down to −170°C (the minimum temperature that can be reached).

When θ_a = 150°C, twins and/or ϵ platelets begin to appear, but are still rather rare.

When θ_a = 110°C, twins, ϵ platelets and stacking faults generalize: plastic deformation at θ_a must be responsible for the great majority of these defects, the twinned and/or ϵ transformed volume fraction appearing to be much higher than that which is observed in a quenched condition at RT (Fig. 7(*a*)). Dislocations are entangled in planar arrangements (Fig. 7(*b*)). All these structures are typical of a rather low SFE at θ_a. On cooling they prove to be far less stable than the structures obtained after deformation at 500°C: planar defects propagate at temperatures as high as −30 to −40°C and their extension is quite appreciable (Fig. 8).

1.4 SPONTANEOUS $\gamma \rightarrow \alpha'$ TRANSFORMATION IN PRESTRAINED CONDITIONS

The variations of intensity of magnetization of Steel 1 strained from ϵ_a = 0 to 30 pct at 110 and 500°C and quenched for 90 min in liquid nitrogen are plotted as a function of ϵ_a in Fig. 9; it can be seen that the stabilization of austenite towards $\gamma \rightarrow \alpha'$ transformation due to prestraining is less efficient if temperature θ_a is close to M_d (110°C) than if θ_a is much higher (500°C). Similar behavior had already been reported by Breedis[8] for ϵ_a higher than about 10 pct.

1.5 ELASTIC STRESS-INDUCED TRANSFORMATION. MECHANICAL PROPERTIES

Specimens of Steel 1 were strained (ϵ_a = 30 pct ± 0.25 pct) at θ_a = 110 and 500°C and then tested in tension between −60 and +150°C. The variations of the macroscopic yield stress σ_y as a function of test temperature θ are plotted in Fig. 10. The yield stress of the steel prestrained at 500°C appears to be higher than the yield stress of the steel prestrained at 110°C in the whole test temperature range.

i) Above 50°C, σ_y decreases "normally" as θ increases and it is impossible to detect any stress-induced $\gamma \rightarrow \alpha'$ transformation at the beginning of the plastic deformation (continuous magnetic measurements); there is only a slight difference between the yield stresses of both conditions.

ii) Below 50°C, this difference is much larger and

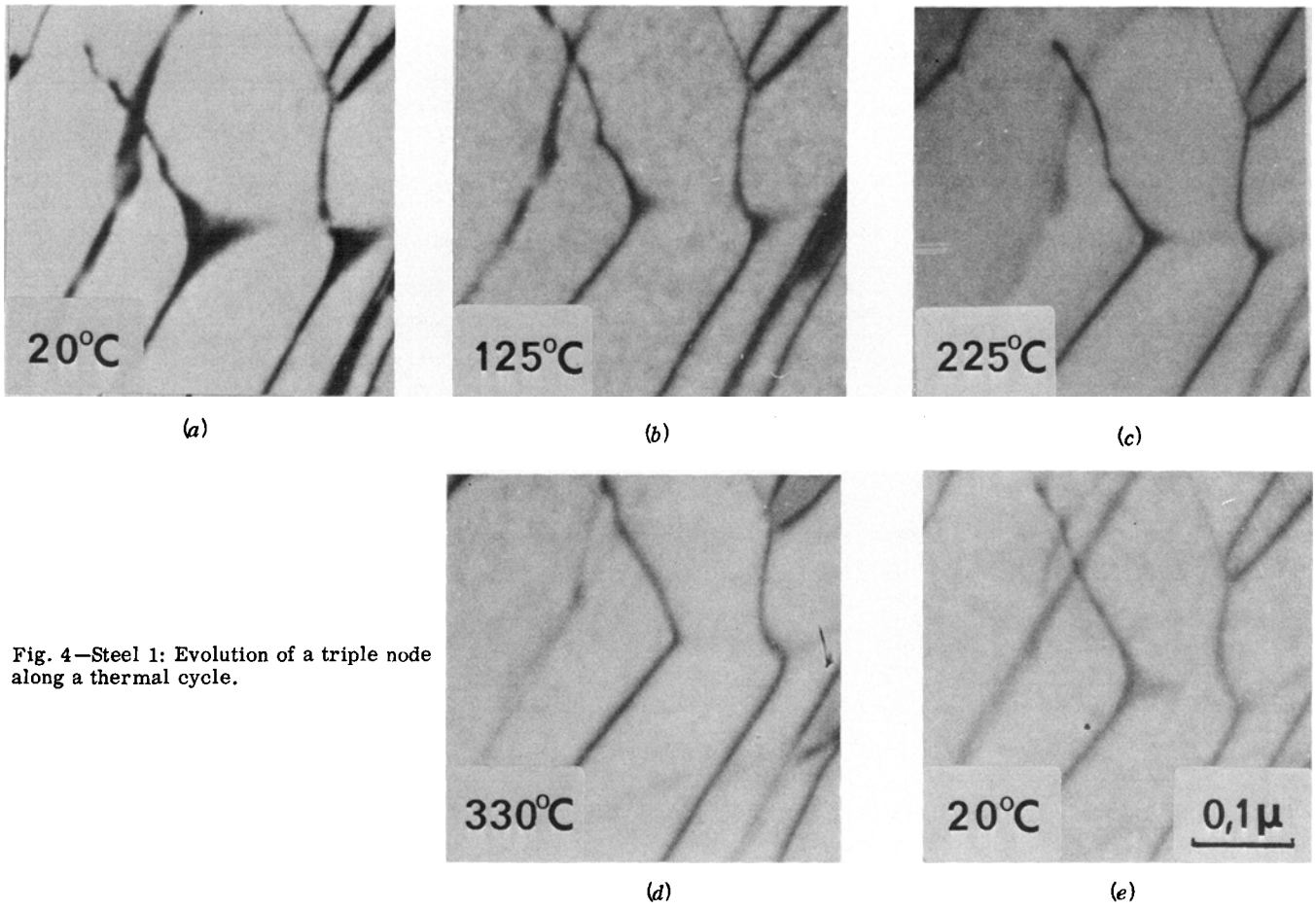

Fig. 4—Steel 1: Evolution of a triple node along a thermal cycle.

$\gamma \rightarrow \alpha'$ transformation starts immediately on yielding in both conditions. Yield starts with the nucleation of a Lüders band.

iii) Finally, the yield stresses decrease with temperature below 50°C in the condition strained at 110°C and below 20°C in the condition strained at 500°C: the transformation-controlled yield stress phenomenon is usually related to this abnormal yield stress-temperature positive sensitivity.

These observations show that the stress-induced $\gamma \rightarrow \alpha'$ transformation is easier if the prestraining of the austenite has been carried out at a temperature closer to M_d.

Finally, a chemical etching just after yielding at RT allows to ascertain—*a posteriori*—the generality of the association between ϵ and/or twins and α' stress-induced martensite in both conditions (Fig. 11). However, the nucleation of α' on preexisting planar defects seems to be a rather rare event (Fig. 12).

2. Steel 2

In view of our observations on a synthetic steel, it was interesting to investigate the behavior of a commercial steel.

2.1 ALLOY STRUCTURE IN THE QUENCHED CONDITION AND TRANSFORMATION TEMPERATURES

M_s ($\gamma \rightarrow \alpha'$) temperature is located between 0 and 10°C and the morphology of the martensite is quite similar to that of steel 1. M_d temperature is approximately 120°C.

Although the instability of austenite at RT prevented any SFE measurements we observed a wide splitting of dislocations, suggesting a rather low SFE value; however, no ϵ martensite could be detected by the electron diffraction technique: both this absence and the lower value of the (M_s, M_d) range suggest a higher SFE for Steel 2 at a given temperature.[11] In addition, the faulted area keeps growing while cooling in thin foils: although these are not equilibrium-defects, it may be inferred that the SFE decreases with temperature, as in Steel 1.

2.2 MODES OF PLASTIC DEFORMATION IN AUSTENITE ABOVE M_d. INFLUENCE OF TEMPERATURE

The structures are similar to those of Steel 1: after a deformation at 500°C (ϵ_a = 18 pct) only equiaxed dislocation cells typical of a high SFE could be observed, while after a deformation at 150°C (ϵ_a = 18 pct), plastic deformation was seen to be partly achieved by mechanical twinning and the propagation of stacking faults. Some ϵ martensite could be identified after ϵ_a = 16 pct at 100°C.

2.3 SPONTANEOUS $\gamma \rightarrow \alpha'$ TRANSFORMATION IN PRESTRAINED CONDITIONS

The variation of intensity of magnetization of Steel 2 strained from ϵ_a = 0 to 20 pct at 150 and 500°C and

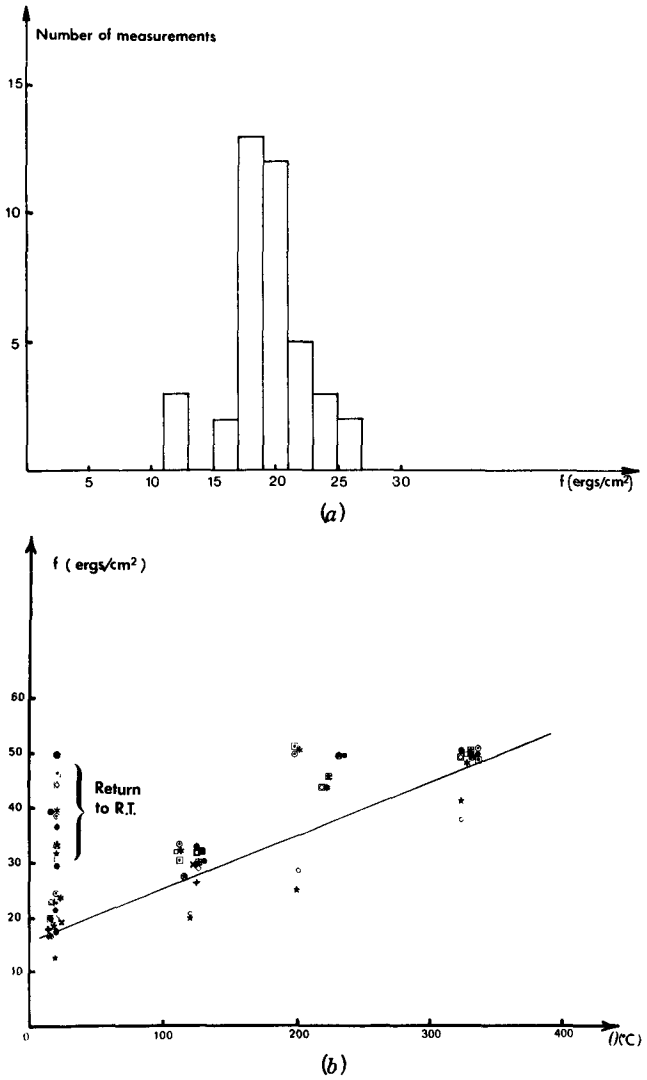

Fig. 5—Steel 1: SFE measurements, (*a*) measurements at *RT*; (*b*) variation of SFE with temperature.

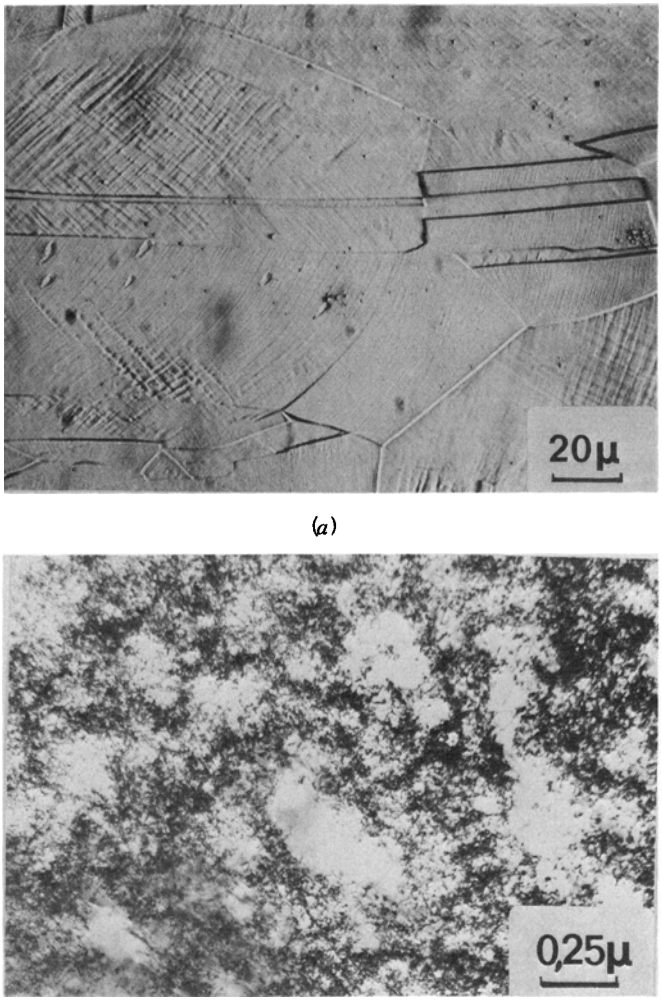

Fig. 6—Steel 1 strained 20 pct at 500°C: deformation structure of the austenite, (*a*) slip lines; (*b*) dislocation cells.

quenched for 2 h in liquid nitrogen are plotted as a function of ϵ_a in Fig. 13; the trend observed in Steel 1 is much more apparent here: $\gamma \rightarrow \alpha'$ transformation is far less stabilized after straining at a temperature close to M_d than after straining at a higher temperature.

2.4 ELASTIC STRESS-INDUCED TRANSFORMATION. MECHANICAL PROPERTIES

In a still more apparent manner than in the case of Steel 1, elastic stress-induced $\gamma \rightarrow \alpha'$ transformation is easier when the prestraining of austenite has been performed at a temperature closer to M_d. In addition, yield points can be observed on tensile curves. Specimens of Steel 2 were strained ($\epsilon_a = 20 \pm 0.25$ pct) at 150, 350, and 500°C (these last two temperatures leading to the same results) and then tested in tension in the range (−40, 200°C). The variations of upper (σ_y^u) and lower (σ_y^l) yield stresses as a function of test temperature θ are plotted in Fig. 14(*a*).

i) Above 100°C, σ_y decreases "normally" as θ increases, no $\gamma \rightarrow \alpha'$ transformation is detected at yielding by continuous magnetic measurement and the difference between the yield stresses of both conditions is less than 5 hbar.

ii) Below 100°C, yield stresses are much lower after straining at 150°C than after straining at 500°C and $\gamma \rightarrow \alpha'$ starts just at yielding. Moreover the yield points are much sharper in the latter case than in the former. There is an "abnormally" positive yield stress-temperature sensitivity.

iii) Finally, we have reported in Fig. 14(*b*) the variations of σ_y^u with ϵ_a at given values of θ and θ_a: σ_y^u stops increasing when ϵ_a exceeds a critical value; the maximum value of σ_y^u decreases with θ_a and θ.

DISCUSSION

1. SFE and Modes of Deformation of Austenite

The following will mainly concern Steel 1 in which SFE measurements were carried out. In a recent survey, Gallagher[37] has discussed the factors which may affect the size of extended dislocation nodes upon changes of temperature. These factors include:

a) The Suzuki effect[38] implying a deviation of the equilibrium concentration of solutes in the fault (hcp) from the concentration of solutes in the matrix (fcc). This effect probably operates in systems where there

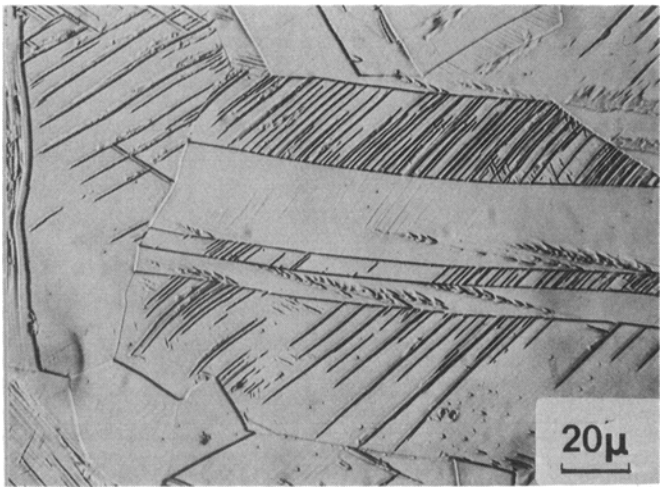

(a)

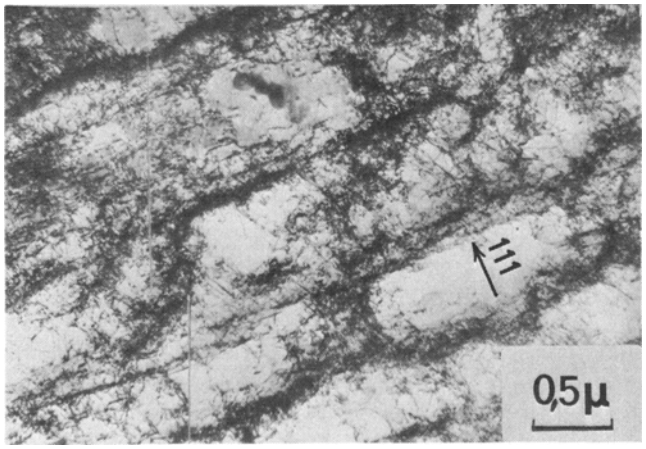

(b)

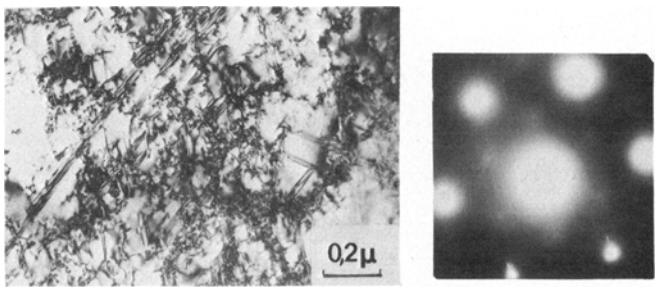

(c)

Fig. 7—Steel 1 strained 20 pct at 110°C: deformation structure of the austenite, (*a*) ϵ platelets and/or mechanical twins; (*b*) dislocation cells; (*c*) ϵ martensite and corresponding (111) diffraction pattern.

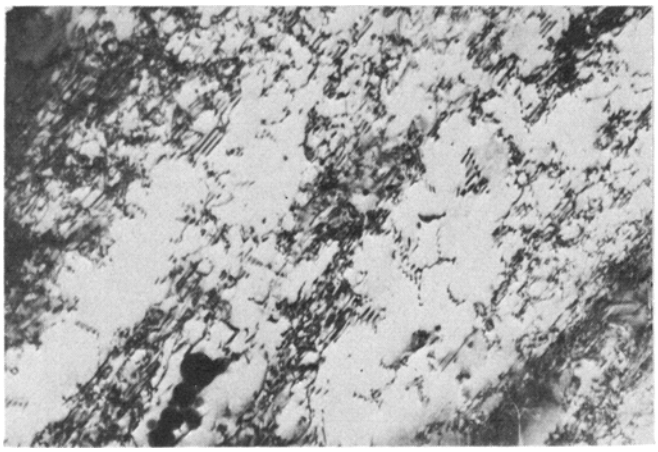

(a)

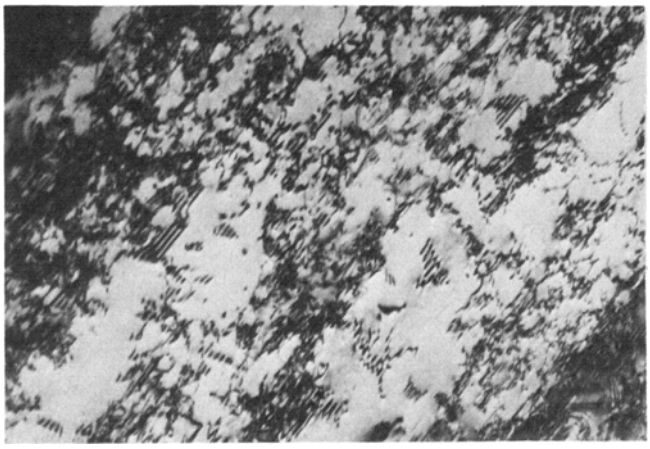

(b)

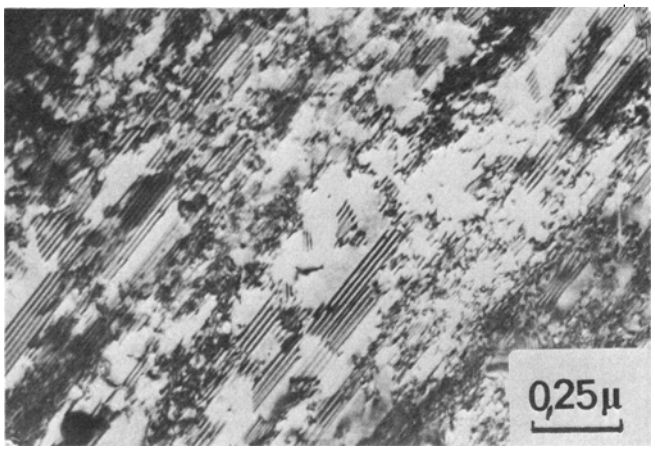

(c)

Fig. 8—Steel 1 strained 20 pct at 110°C: evolution of the structure on the cooling stage: (*a*) 20°C; (*b*) −35°C; (*c*) −169°C.

is a strong dependence of SFE upon composition, which is the case of stainless steels.[37]

b) Segregation of interstitial atoms on partial dislocations.

c) Thermally activated unpinning of partial dislocations.

d) A true dependence of the SFE on temperature.

The solute concentration being very probably the same in the fault as in the matrix at RT, the Suzuki effect should lead to a decrease of the SFE with higher temperature because of increased diffusivities. Therefore this effect is unable to explain the observed changes.

Effect *b* slows down the displacements of dislocations at temperatures where it occurs, but cannot produce a variation of the SFE.

Effect *c* should involve an irreversible decrease or increase of faulted area on temperature increase and not only a decrease, as asserted by Gallagher.[37] Furthermore, it would not explain the strong decrease of SFE with temperature below RT, as observed by ourselves.

As a consequence, we think that effect *d*, that is a

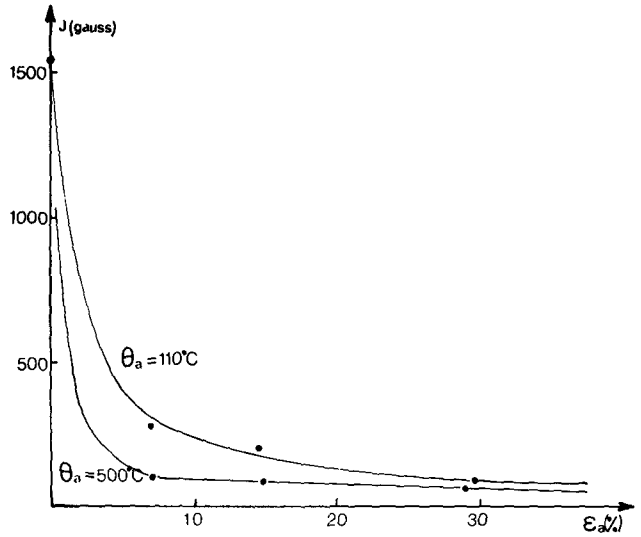

Fig. 9—Steel 1: Spontaneous $\gamma \rightarrow \alpha'$ transformation on pre-strained conditions. Intensity of magnetization vs amount of previous strain.

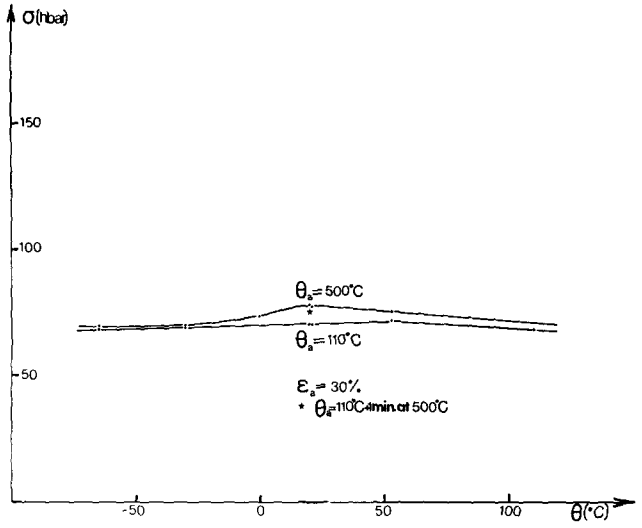

Fig. 10—Steel 1: Yield stresses of pre-strained conditions vs test temperature for ϵ_a = 30 pct.

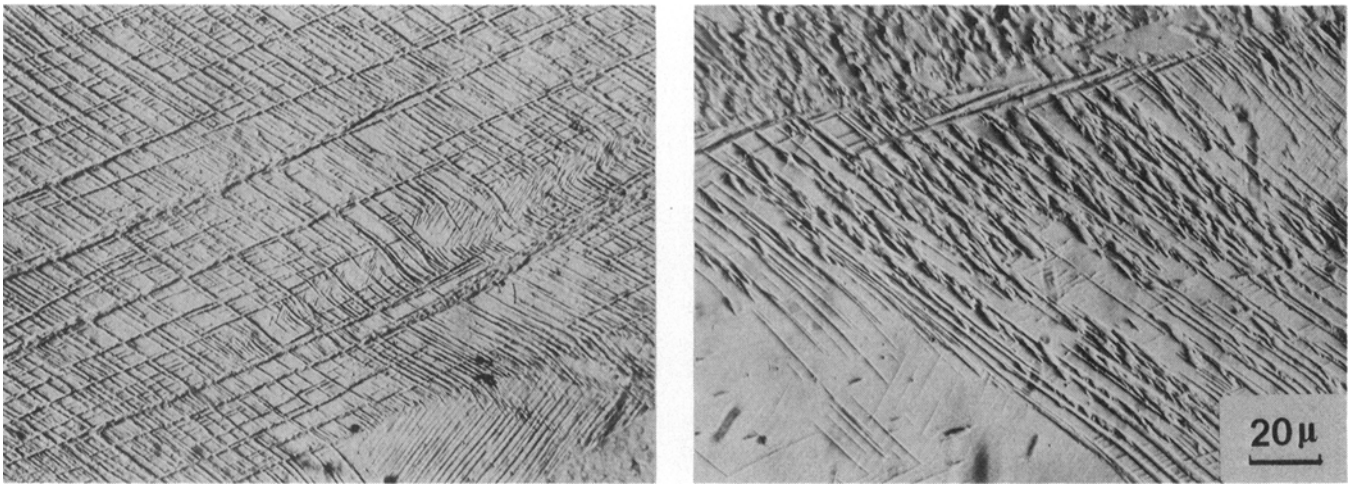

(a) (b)

Fig. 11—Steel 1: Deformation structures, (*a*) 20 pct at 500°C + yield at *RT* (in Lüders band); (*b*) 20 pct at 110°C + yield at *RT* (in Lüders band).

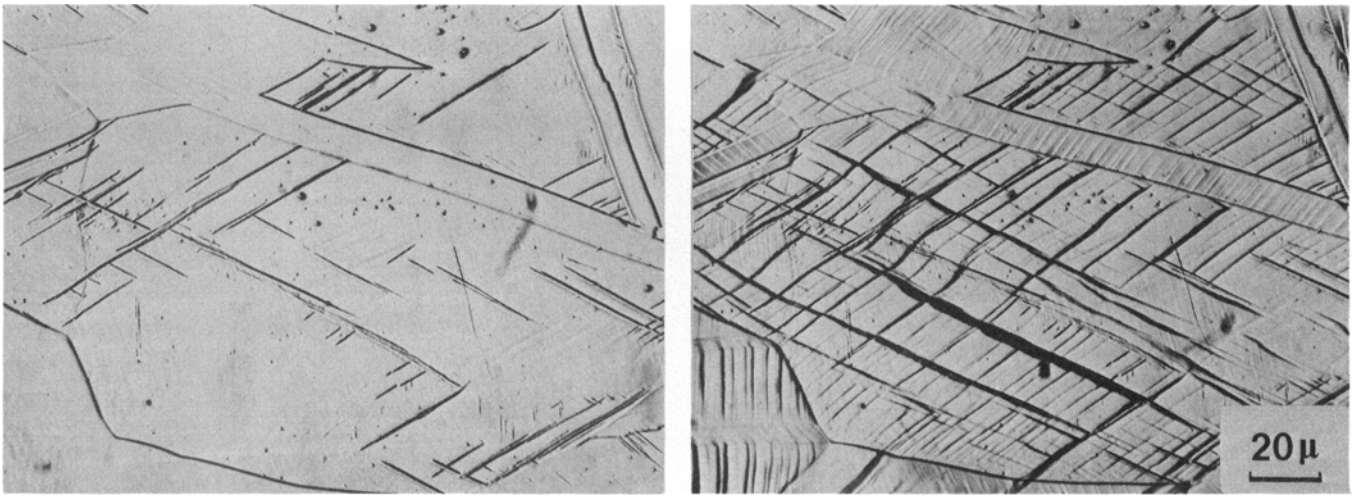

(a) (b)

Fig. 12—Steel 1: Deformation structures, (*a*) 23 pct at 150°C (plane defects revealed by etching); (*b*) same area + yield at *RT* (α' martensite and new plane defects revealed by relief effects).

true dependence of the SFE on temperature, is prevailing on heating (which does not necessarily mean that measured values of SFE are true values, especially at high temperatures).

This conclusion is consistent with i) the occurrence of a $\gamma \rightarrow \epsilon$ transformation, the corresponding Gibbs free energy variation $\Delta G^{\gamma \rightarrow \epsilon}$ of which is dependent on temperature and is related to the SFE,[11,39] ii) the peculiar influence of temperature on plastic deformation modes in austenite above M_d[8,10,28,30] and iii) similar recent results obtained on stainless steels.[11,12,40,41] Furthermore, according to these last results, there would be an increase of SFE with temperature which is perfectly reversible below RT[11,12,40] and mostly reversible in the (20, 350°C) range[41] on stainless steels of neighboring compositions but containing only traces of carbon. This last element might thus be inferred to be greatly responsible, through effect *b*, for the irreversibility that we observed.

With Steel 2, the influence of temperature on the modes of deformation of austenite above M_d and the extension of (nonequilibrium) stacking faults on cooling suggest that the SFE increases likewise with temperature.

2. Nucleation Processes in Stress-induced and Spontaneous $\gamma \rightarrow \alpha'$ Transformations

The interrelations between stress, defects in austenite, and phase transformation will now be examined as they may provide some information on the processes involved.

In the above investigation, a correlation between two series of experimental results has been noted:

i) The substructure induced by a prestraining of austenite above M_d, such as may be observed at RT.

ii) The stability of austenite towards elastic stress-induced and spontaneous $\gamma \rightarrow \alpha'$ transformations, this stability being higher if θ_a is closer to M_d.

This correlation suggests that $\gamma \rightarrow \alpha'$ transformation depends i) on the nature and arrangement of defects in austenite at RT after prestraining ii) and/or on their ability to evolve when the temperature is lowered or the applied stress increased. A comparative study of the nature and ability of evolution of structures can then allow to determine the factors which are most favorable to transformation. For convenience, the structures induced by straining at 110 to 150 and 500°C will be henceforth referred to as condition 1 and condition 2 respectively.

i) concerning the nature and arrangement of defects in austenite, condition 1 contains plane defects (twins, ϵ platelets, stacking faults) whereas condition 2 does not. In addition, according to Breedis,[8] internal stresses should be higher in condition 1 because of the planar arrangement of split dislocations; this last hypothesis will be discarded in the following.

ii) concerning the ability of structures to evolve,

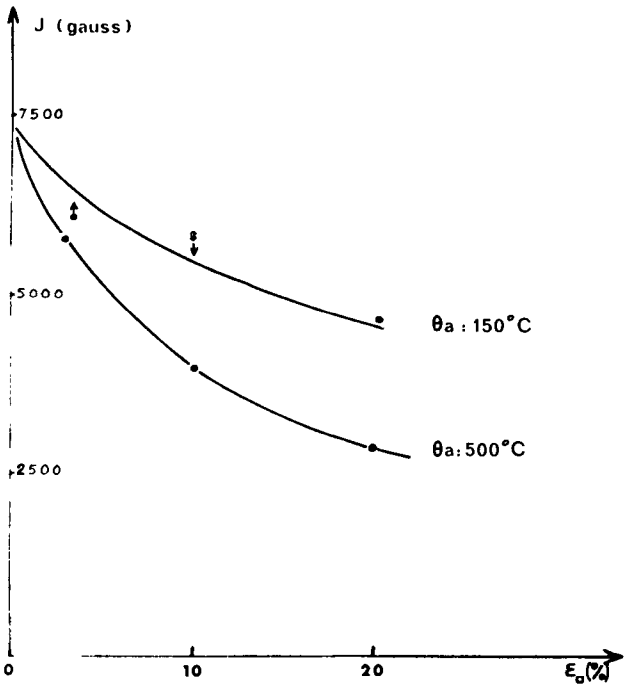

Fig. 13—Steel 2: Spontaneous $\gamma \rightarrow \alpha'$ transformation on prestrained conditions. Intensity of magnetization vs amount of previous strain.

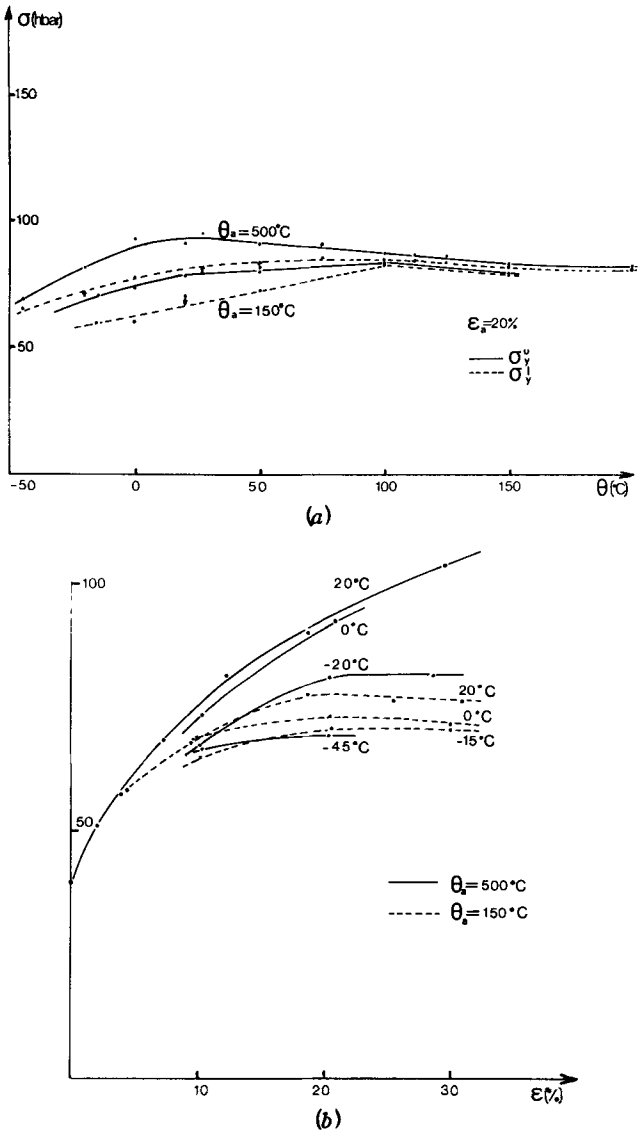

Fig. 14—Steel 2: Mechanical properties of pre-strained conditions, (*a*) yield stress vs test temperature for ϵ_a = 20 pct; (*b*) yield stress vs amount of previous strain for various test temperatures.

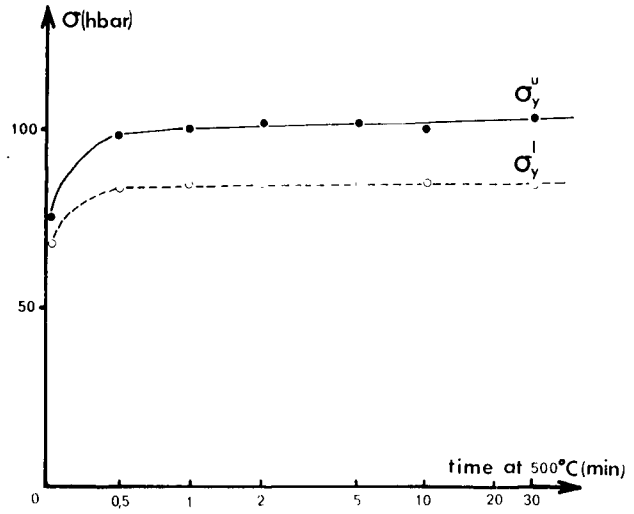

Fig. 15—Steel 2: Condition 1 (30 pct at 150°C) aged at 500°C: yield stress vs aging time.

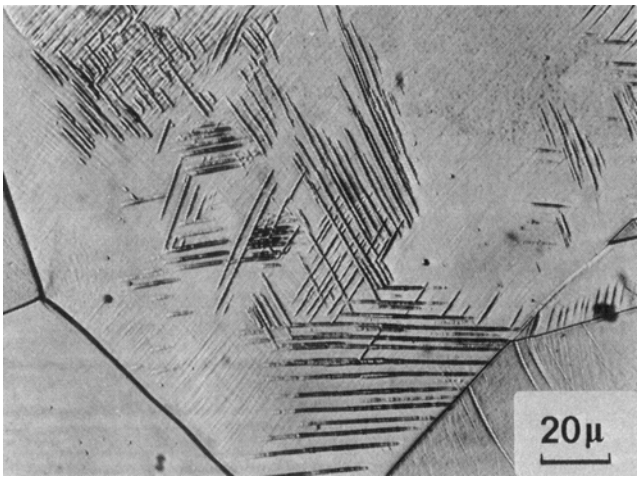

Fig. 16—Steel 1: Structure of condition 1 (20 pct at 110°C) aged for 1 mn at 500°C.

we think that existing or new planar defects propagate more easily in condition 2 than in condition 1 when the stress is increased or the temperature lowered. This can be explained by the lower yield stress in condition 1, already mentioned (Figs. 10 and 14(*a*)), and the lower stability of condition 1 towards the extension of faulted area when cooled as thin foil (Fig. 8). The segregation of impurities (carbon) on partial dislocations and the resulting pinning inferred from the results of SFE measurements might explain this behavior if they are more complete in condition 2 than in condition 1, which is likely to occur (see Appendix 1). The entanglement of perfect dislocations in cells in condition 2 might also contribute to this difference.

The preceding analysis suggests that the nucleation of stress-induced $\gamma \rightarrow \alpha'$ transformation is easier i) if plane defects are in greater number ii) and/or if existing or new plane defects propagate more freely.

Under the assumptions of the first hypothesis, stress-induced α' martensite would nucleate only on preexisting plane defects ("static nucleation"). However, the transformation mechanism involved, perhaps a homogeneous elastic straining of ϵ platelets under stress, is difficult to imagine. From an experimental standpoint, it would be difficult to explain the occurrence of the transformation in condition 2 where plane defects do not appear. In addition, we showed that static superficial nucleation is a rather rare event. Finally, the volume fraction twinned and/or transformed into ϵ martensite appears to be much higher after yielding (which occurs by the nucleation of a Lüders band, Fig. 11(*b*)) than before (Fig. 7(*a*)) in condition 1.

It may then be concluded that the nucleation stress of elastic stress-induced $\gamma \rightarrow \alpha'$ transformation is, at temperatures where this type of transformation occurs (near M_s), directly dependent on the stress necessary to propagate plane defects in austenite. This conclusion is consistent with the generality *a posteriori* of the association between α' and plane defects (Fig. 11).

To confirm this point, we carried out the following experiment. If a specimen of Steel 2 is strained 30 pct at 150°C and rapidly heated in a salt bath to 500°C (or 350°C), the yield stress rises readily to the level corresponding to direct straining at 500°C (Fig. 15). The same phenomenon occurs in Steel 1, although not as completely (Fig. 10). Furthermore, electron and optical microscopies show that planar defects and particularly ϵ martensite have not disappeared after this aging (Fig. 16). Thus, considering the rapidity of the change, we feel that the only explanation is to be found in a segregation of impurities on dislocations during aging, which reduces the ability of the planar defects to propagate under an applied stress. Moreover, this experiment discards the hypothesis according to which the differences between the behaviors of both conditions might be explained by differences of internal stresses: the aging time is too short to allow a relaxation of these stresses.[8]

Regarding the spontaneous $\gamma \rightarrow \alpha'$ transformation, a similar analysis may allow to relate the nucleation processes to the propagation of plane defects in austenite, internal stresses (which depend on SFE) being considered alone.

3. Mechanical Properties

The influence of the test temperature on the yield stress will now be discussed. As emphasized in the preceding section, the prior propagation of plane defects is a necessary condition for the occurrence of elastic stress-induced $\gamma \rightarrow \alpha'$ transformation; the yield stress above M_s is then always controlled by the interactions of dislocations with impurities and other dislocations, whether the transformation takes place or not.

Regarding condition 1, where segregation is very light, interactions between dislocations are only to be considered. Saada treated the problem in the case of perfect dislocations in fcc single crystals;[45] his results also apply in the case of turbulent flow in fcc polycrystals[42] here considered. Fontaine[48] showed that, when the SFE (f) is low enough, the deformation is more easily carried out by the propagation of stacking faults. The transition occurs when the flow stress corresponding to this latter case, Eq. [1] becomes lower than the flow stress estimated by Saada, Eq. [2], that is to say when:

$$[1]\quad \sigma_y^1 = \frac{\mu \mathbf{b}_s}{4l} + \frac{f}{\mathbf{b}_s} < \sigma_y^2 = \frac{\mu \mathbf{b}}{4l} \quad [2]$$

where $\mathbf{b}$, $\mathbf{b}_s$ are the Bürgers vectors of the perfect and

imperfect dislocations (here $b = b_s\sqrt{3}$) and l is the mean free path between dislocations crossing a slip plane: f decreasing with θ, a decrease of σ_y with θ below the transition temperature may be expected (Fig. 17).

It follows that:

$$\frac{d\sigma_y^1}{d\theta} = \frac{b_s}{4l}\frac{d\mu}{d\theta} + \frac{1}{b_s}\frac{df}{d\theta}$$

$$\simeq \sigma_y^{max}\frac{b_s}{b}\frac{1}{\mu}\frac{d\mu}{d\theta} + \frac{1}{b_s}\frac{df}{d\theta}$$

With $b_s = 1.5\times10^{-8}$ cm, $\frac{1}{\mu}\frac{d\mu}{d\theta} = 7\times10^{-4}$ per deg C, $\frac{df}{d\theta} \simeq 0.1$ ergs per sq cm per deg C, $\sigma_y^{max} = 70$ hbar (Steel 1) and $\sigma_y^{max} = 80$ hbar (Steel 2), $\frac{d\sigma_y^1}{d\theta} = 3.8$ hbar per 100°C (Steel 1) and $\frac{d\sigma_y^1}{d\theta} = 3.4$ hbar per 100°C (Steel 2).

These values are consistent with the experimental results (4 hbar per 100°C in the range (−50, +50°C) on Steel 1 and 3.5 hbar per 100°C in the range (0, 100°C) on Steel 2).

Finally, considering the direct dependence of ϵ_a on l, it may be noted that this model can explain an abrupt decrease of $d\sigma_y/d\epsilon_a$ as ϵ_a exceeds a transition value, but not a constant value for σ_y above this transition as is actually observed (Fig. 14(*b*)).

Since we are concerned with macroscopic yield stresses, we must discuss a complementary mechanism: it may be that the crossing of two nonparallel planar defects could be made still easier by the formation of α' martensite along their intersection.[11,12] Once started, the movement of planar defects would then be accelerated by this mechanism, which would lead to a lower macroscopic yield stress and would enhance the positive yield stress-temperature sensitivity. We feel that this mechanism is more likely to be operative at the lowest temperatures where the $\gamma \rightarrow \alpha'$ transformation is easiest.

Regarding condition 2, the effect of segregation can probably account for the increment of yield stress. The resulting hardening, however, is very difficult to estimate. In addition, the positive yield stress-temperature sensitivity at the lowest temperatures (line 4, Fig. 17) rises another problem: a possible mechanism might be the assistance of unpinning under stress by the repulsion between pinned partial dislocations when the SFE has become low enough.

It is worth recalling here that Zackay *et al.*[47] have attributed the hardening of TRIP steels to the transgranular precipitation of Mo_2C carbides during the prestraining of austenite near 500°C. In the steels studied in this work, a careful examination on thin foils did not show any precipitation. The straining conditions, however, were rather different.

CONCLUSION

1) On both steels studied, the temperature θ_a of previous deformation of austenite above M_d strongly influences the nature and arrangement of defects such as they are observed at RT; if θ_a is close to M_d, planar defects, *i.e.*, stacking faults, mechanical twins and ϵ martensite platelets, are very abundant (condition 1); if θ_a is higher (500°C), dislocation cells can only be observed on both steels (condition 2). In addition, the ability of existing or new defects to propagate with either an applied stress or a temperature decrease is larger in condition 1 than in condition 2.

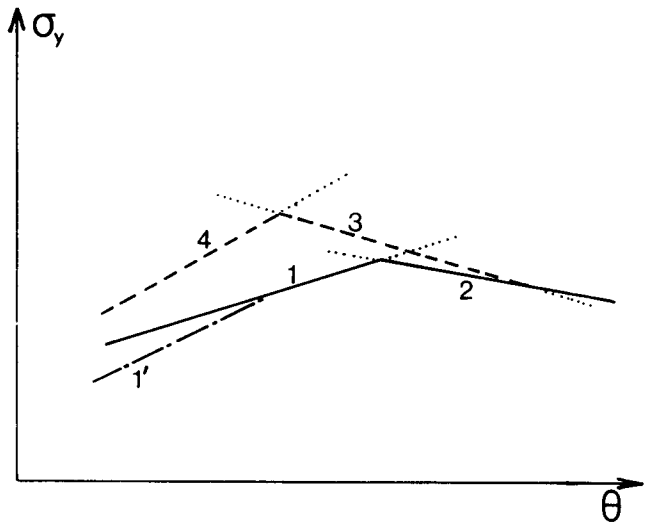

Fig. 17—Schematic variations of yield stress with test temperature.

2) These differences may be simply explained by the value of the intrinsic stacking fault energy (SFE) of austenite: SFE is low at RT (18 ergs per sq cm) and increases steadily with temperature (≃0.1 ergs per sq cm per deg C). SFE measurements have also evidenced the occurrence of a segregation of impurity atoms (probably carbon) on dislocations. This segregation is more intense in condition 2 than in condition 1 and so would explain the fact that defects propagate more easily in condition 1.

3) The yield stress of both steels in the (M_s, M_d) range increases with θ_a at a given value of ϵ_a. This dependence is most noticeable when the yield stress is "controlled" by the $\gamma \rightarrow \alpha'$ martensitic transformation, *i.e.*, at low enough testing temperatures. In addition, the stability of austenite towards spontaneous $\gamma \rightarrow \alpha'$ transformation is lessened if previous straining has been carried out closer to M_d.

4) It may then be deduced that low temperature prestraining of austenite promotes elastic stress-induced $\gamma \rightarrow \alpha'$ transformation between M_s and M_d and spontaneous $\gamma \rightarrow \alpha'$ transformation below M_s, as compared with higher temperature prestraining. Considering the nature and structure of defects present in both conditions, it is concluded that the nucleation stress of $\gamma \rightarrow \alpha'$ transformation is the stress necessary to propagate planar defects in austenite, which would ensure the creation and propagation of transformation dislocations through still poorly understood mechanisms. The nucleation process thus appears to be dynamic.

APPENDIX I

An Evaluation of Carbon Atoms Segregation on Dislocations in Austenite

Let C_0 be the mean concentration of carbon atoms in the metal.

The equilibrium concentration C_M is given by $C_M = C_0 \exp(-W_m/kT)$ (below saturation) and the concentration $C - C_0$ of atoms having arrived on dislocations at time t is $C - C_0 = \pi C_0 [3D|W_m|t/b^2 kT]^{2/3}$ if $C \ll C_M$, where $W_m \simeq 0.23$ eV [43] is the interaction energy between these atoms and dislocations and $D \simeq 0.25 \exp(-35{,}000/RT)$ cm^2 per s (Ref.44) is the diffusion coefficient of carbon atoms in Fe_γ.[42]

For $T = 400$ K (condition 1) and $t \simeq 1000$ s (approximate straining time), $C \simeq 3C_0$ which is very low and much less than saturation.

For $T > 600$ K (condition2), the time necessary to reach equilibrium is less than 1 s: the concentration at RT after straining at $T > 600$ K is then close to equilibrium concentration at 600 K, say about $100C_0$, which is much higher and close to saturation.

ACKNOWLEDGMENTS

The author is grateful to Dr. F. Lecroisey and Dr. A. Pineau for stimulating discussions. This work was performed under financial support of the C.E.C.A. (Communauté Européenne du Charbon et de l'Acier).

REFERENCES

1. E Scheil. *Zeit. Anorg. Allgem. Chem.*, 1932, vol. 207, p. 21.
2. D. Fahr: Thesis, University of California, Berkeley, California, 1969.
3. A. W. McReynolds: *J. Appl. Phys.*, 1949, vol. 20, p. 896.
4. S. A. Kulin, M. Cohen, and B. L. Averbach: *J. Metals*, 1952, vol 4, p. 661.
5. J. F. Breedis and W. D. Robertson: *Acta Met.*, 1963, vol. 11, p. 547.
6. R H. Richman and G. F. Bolling: Ford Report, May 1969.
7. D. Bhandarkar, V. F. Zackay, and E. R. Parker: *Met. Trans.*, 1972, vol. 3, p. 2619.
8. J. F. Breedis. *Acta Met.*, 1965, vol. 13, p. 239.
9. D. Rousseau, G. Blanc, R. Tricot, and A. Gueussier: *Mem. Sci. Rev. Met.*, 1970, vol. 67, p. 315.
10. B. Thomas: *Met. Corr. Ind.*, 1969, vol. 532, p. 405.
11. F. Lecroisey: Thesis, Faculté des Sciences, Nancy, France, 1971.
12. F. Lecroisey and A. Pineau: *Met. Trans.*, 1972, vol. 3, p. 387.
13. R. Lagneborg: *Acta Met*, 1964, vol. 12, p. 823.
14. W. O. Binder: *Met. Progr.*, 1950, vol. 58, p. 201.
15. B. Cina: *J. Iron Steel Inst.*, 1954, vol. 177, p. 406.
16. B. Cina. *Acta Met.*, 1958, vol. 6, p. 748.
17. C. J. Guntner and R. P. Reed: *Trans. ASM*, 1962, vol. 55, p. 399.
18. D. Mugnier Thesis, Faculté des Sciences, Grenoble, France, 1964.
19. R. P. Reed: *Acta Met.*, 1962, vol. 10, p. 865.
20. J. Dash and H. M. Otte: *Acta Met.*, 1963, vol. 11, p. 1169.
21. J. F. Breedis: *Trans. TMS-AIME*, 1964, vol. 230, p 1583.
22. H. M. Otte: *Acta Met.*, 1957, vol. 5, p. 614.
23. A. J. Goldman, W. D. Robertson, and D. A. Koss: *Trans. TMS-AIME*, 1964, vol. 230, p. 140.
24. J. A. Venables: *Phil. Mag*, 1962, vol. 7, p. 135.
25. H. Schumann and H. J. Von Fircks: *Arch. Eisenhuttenw.*, 1969, vol. 40, p. 561.
26 P. M. Kelly and J. Nutting: *J. Iron Steel Inst.*, 1961, vol. 197, p. 199.
27. P. M. Kelly: *Acta Met.*, 1965, vol. 13, p. 635.
28. M. J. Whelan: *Proc. Roy. Soc.*, 1958, vol. 249, p. 114.
29. P. R. Swann: *Corr.*, 1963, vol. 19, p. 102t.
30, D. L. Douglass, G. Thomas, and W. R. Roser: *Corr.*, 1964, vol. 20, p. 15t.
31. A. J. Bogers and W. G. Burgers: *Acta Met.*, 1964, vol. 12, p. 255.
32. J. A. Venables: "Deformation Twinning", p. 77, Gordon and Breach, N. Y., 1964.
33. L. M. Brown and A. R. Tholen: *Dis. Faraday Soc.*, 1964, vol. 38, p. 35.
34. F. Abrassart, F. Lecroisey, and A. Pineau: *Mem. Sci. Rev. Met.*, 1966, vol. 66, p. 805.
35. J. F. Breedis and W. D. Robertson: *Acta Met.*, 1962, vol. 10, p. 1077.
36. B. Thomas: *Met. Corr. Ind.*, 1969, vol. 531, p. 363.
37. P. C. J. Gallagher: *Met. Trans.*, 1970, vol. 1, p. 2429.
38. H. Suzuki: "Dislocations and Mechanical Properties of Crystals", p. 853, Wiley, N. Y., 1956.
39. T. Ericsson: *Acta Met.*, 1966, vol. 14, p. 853.
40. F. Lecroisey and B. Thomas. *Phys. Stat. Sol.*, 1970, vol. A2, p. K217.
41. R. M. Latanision and A. W. Ruff, Jr.: *Met. Trans.*, 1971, vol. 2, p. 505.
42. J. Friedel: "Dislocations", pp. 273, 355, 405, Pergamon Press, 1967.
43. G. S. Ansell and A. Arrott: *Trans. TMS-AIME*, 1963, vol. 227, p. 1080.
44. Y. Adda and J. Philibert: "La Diffusion dans les Solides", p. 1166, Presses Universitaires de France, Paris, 1966.
45. G. Saada: Thesis, Faculté des Sciences, Paris, France, 1960.
46. G. Fontaine *J. Phys.*, 1966, vol 27, p. 201.
47. J. A. Hall, V. F. Zackay, and E. R. Parker: *Trans. ASM*, 1969, vol. 62, p. 965.